MTP-AERO-62-35
April 16, 1962

37 p.

GEORGE C. MARSHALL SPACE FLIGHT CENTER

HUNTSVILLE, ALABAMA

A THEORETICAL INVESTIGATION OF THE EFFECTS OF THE CONFIGURATIVE DESIGN OF A SPACE VEHICLE ON ITS STRUCTURAL BENDING FREQUENCIES AND AERODYNAMIC STABILITY

By

Nathan L. Beard

GEORGE C. MARSHALL SPACE FLIGHT CENTER

MTP-AERO-62-35

A THEORETICAL INVESTIGATION OF THE EFFECTS OF THE CONFIGURATIVE DESIGN OF A SPACE VEHICLE ON ITS STRUCTURAL BENDING FREQUENCIES AND AERODYNAMIC STABILITY

By Nathan L. Beard

ABSTRACT

Six space vehicle configurations are investigated to determine their relative merits as pertaining to rigid body control characteristics and structural bending frequencies. Rigid body theory was used to illustrate the factors which govern the stability of a vehicle in flight. The aerodynamic moment coefficient (C_1), which is one of these factors, was determined from slender body theory. The thrust moment coefficient (C_2) was determined for each vehicle and the ratio C_2/C_1 was chosen as the control-stability parameter to be used in the comparison of the vehicles. The bending frequency parameter chosen was $f_n/\sqrt{C_1}$. It was observed that long slender vehicles exhibit better control characteristics than short vehicles with small length-to-diameter ratios, but the short vehicles, in turn, have higher bending frequencies. For conical, single-diameter cylindrical, and dual-diameter cylindrical vehicles with the same approximate length, the conical vehicle exhibits better bending and control characteristics than the other two, while the single-diameter cylindrical is better than the dual-diameter cylindrical vehicle.

An arbitrary equation was developed for the weighted diameter, D_w, of the vehicles, and a vehicle shape parameter was chosen. This parameter varies nearly linearly with the structural bending frequencies of the vehicles.

GEORGE C. MARSHALL SPACE FLIGHT CENTER

MTP-AERO-62-35

April 16, 1962

A THEORETICAL INVESTIGATION OF THE EFFECTS OF THE CONFIGURATIVE DESIGN OF A SPACE VEHICLE ON ITS STRUCTURAL BENDING FREQUENCIES AND AERODYNAMIC STABILITY

by

Nathan L. Beard

DYNAMICS ANALYSIS BRANCH
AEROBALLISTICS DIVISION

TABLE OF CONTENTS

TABLES

LIST OF ILLUSTRATIONS

DEFINITION OF SYMBOLS

a	radius of propellant.
h	height of propellant in tank.
a_o	gain factor of attitude channel.
a_1	coefficient of control damping.
F	thrust of engine.
I_{CG}	effective moment of inertia of total vehicle about its C. G.
k	radius of gyration of vehicle about C. G.
m	mass of vehicle.
$\bar{X}_E$	coordinate of swivel point.
$\bar{X}_{IR}$	coordinate of center of instantaneous rotation.
f_n	bending frequency of the nth mode.
C_1	aerodynamic restoring moment coefficient.
C_2	thrust moment coefficient.
C_p	center of pressure.
α	angle of attack at C. G.
β	deflection of swivel engine relative to center line of vehicle.
q	dynamic pressure.
D	diameter of vehicle airframe.
D_o	diameter of base of vehicle
λ	D/D_o
N'	normal lift coefficient.
L	length of vehicle.
t	average thickness of skin of vehicle.
D_w	weighted diameter of vehicle.
l_n	length of nth section of vehicle.
EI	stiffness of vehicle.
m'	mass distribution.

GEORGE C. MARSHALL SPACE FLIGHT CENTER

MTP-AERO-62-35

A THEORETICAL INVESTIGATION OF THE EFFECTS OF THE CONFIGURATIVE DESIGN OF A SPACE VEHICLE ON ITS STRUCTURAL BENDING FREQUENCIES AND AERODYNAMIC STABILITY

by Nathan L. Beard

SUMMARY

A vibration analysis of six space vehicle configurations was conducted to determine the first three bending modes and their corresponding frequencies. Rigid body theory was used to illustrate the factors which govern the stability of a vehicle in flight. The aerodynamic moment coefficient (C_1), which is one of these factors, was determined from slender body theory. The thrust moment coefficient (C_2) was determined for each vehicle and the ratio C_2/C_1 was chosen as the control-stability parameter to be used in the comparison of the vehicles. The bending frequency parameter chosen was $f_n/\sqrt{|C_1|}$.

It was found that vehicles with large L/D ratios exhibited higher C_2/C_1 values, or better control characteristics than vehicles with small L/D ratios; but the short vehicles, in turn, have higher bending frequencies. For conical, single-diameter cylindrical, and dual-diameter cylindrical vehicles with the same approximate length, the conical vehicle exhibits more favorable bending and control characteristics than the other two, while the single-diameter cylindrical is better than the dual-diameter cylindrical vehicle.

An arbitrary equation was developed for the weighted diameter, D_w, of the vehicles, and a vehicle shape parameter was chosen. This parameter varies nearly linearly with the structural bending frequencies of the vehicles.

I. INTRODUCTION

This investigation was conducted primarily for the purpose of obtaining information relative to the configurative design of space vehicles with emphasis placed on obtaining larger structural bending frequencies. It is desirable for space vehicles to have large natural bending frequencies from the stability point of view. For instance, when the first bending mode frequency is approximately the same as the control or fuel sloshing frequencies, interaction between their vibrational modes can bring about control saturation and possibly the destruction of the vehicle; therefore, it becomes necessary to vary certain parameters to provide a frequency gap between these modes. The control frequency may be varied by the slection of different gain factors a_o, a_1, b_o, and g_2 in the control circuit, which are functions of time only, while the sloshing frequency can be varied by the proper choice of the tank form and the height-to-radius ratio, h/a, where h is the height of the fuel in the tanks. With these considerations in mind, it is evident that the space vehicle with the higher first mode natural bending frequency offers a more expanded or wider range from which to choose the gain factors and h/a parameter.

The stability of a vehicle from the aerodynamic point of view depends upon the magnitude and sign of C_2/C_1. The more positive this ratio the better is the stability of the vehicle. The thrust moment coefficient, generally, is positive; however, when the center of pressure is forward of the center of gravity of the vehicle, C_1 is negative. This indicates that a destabilizing moment acts about the center of gravity of the vehicle.

The following analysis of six different vehicle configurations shows their favorable and unfavorable qualities pertaining to the parameters mentioned above.

II. DESCRIPTION

Six vehicle configurations were considered in this analysis. Five of these were chosen as reasonable designs for space vehicles, while the Saturn C-1 was selected as the standard in this study. Configurations 2, 3, and 5 were chosen with the same base diameter and approximate length; however, the overall shape of each was varied to determine the effects this would have on the aerodynamic stability and the structural bending frequencies. One large L/D and one small L/D vehicle was chosen (Vehicles 1 and 4) to contrast the stability and bending characteristics. The Saturn C-1 was chosen, as configuration 0, to be compared with the other five since it had at least one characteristic of each vehicle. Each of the vehicles was idealized as follows:

1. The vehicles empty weight was derived only from the structural weight of its skin.

2. The skin thickness of each vehicle was assumed to be constant throughout its length.

3. All of the vehicles were assumed to be constructed from an aluminum alloy with a density of 0.0975 pounds per cubic inch.

4. The length, diameter, and thickness of the five vehicles chosen as reasonable designs were determined so as to provide a structural weight and internal capacity equal to that of the Saturn vehicle C-1.

5. The nose cones were given a slope identical to that of the Saturn Vehicle (15°, half vertex angle).

6. Each vehicle was filled completely with water to simulate fuel.

Hereafter the Saturn vehicle will be referred to as model number 0 while the other five configurations will be referred to as model numbers 1, 2, 3, 4, and 5. These configurations are shown in Figure 2.

Since the internal volume and structural weight of each vehicle was to be identical to that of vehicle number 0, their length and thickness could be easily calculated from the equations for the volume and surface areas of a cone and cylinder. This data is given in Table I.

Next, the mass distributions, empty and full were plotted as shown in Figures 11 through 16. By using a modified Stodola method (c. f. Reference 3) in conjunction with the IBM 7090 computer, the following data were obtained:

1. The deflection curves for the first three bending modes.
2. The natural bending frequencies corresponding to each of these modes.
3. The center of gravity of the missile.
4. The mass moment of inertia about the center of gravity.
5. The total mass of the missile.

First, the three bending modes were plotted as shown in Figures 2 through 7. The center of instantaneous rotation for each vehicle was determined from the relation:

$$\bar{X}_{IR} = -\frac{k^2}{\bar{X}_E} = -\frac{I_{CG}}{m\bar{X}_E} \qquad (1)$$

where k is the radius of gyration about the vehicle's C. G. and its square is equal to the mass moment of inertia about the center of gravity, $I_{C.G.}$, divided by the total mass, m. The distance from the center of gravity of the vehicle to the swivel point of the engines is denoted by $\bar{X}_E$.

The center of pressure, C_p, is given by the relation:

$$C_p = \frac{\int_{-\frac{L}{2}}^{\frac{L}{2}} \lambda \lambda' \bar{x} \, dx}{\int_{-\frac{L}{2}}^{\frac{L}{2}} \lambda \lambda' \, dx} \tag{2}$$

where $\lambda = \frac{D_{(x)}}{D_o}$ and $D_{(x)}$ is the diameter of the vehicle as a function of x. The diameter at the base of the vehicle is denoted by D_o.

The normal lift coefficient, N', was obtained from the relation:

$$N' = \pi q D_o^2 \int_{-\frac{L}{2}}^{\frac{L}{2}} \lambda \lambda' \, dx = \frac{\pi}{2} q D_o^2 \tag{3}$$

where q is the dynamic pressure.

The aerodynamic restoring moment coefficient, C_1, was calculated from the relation:

$$C_1 = \frac{\pi q D_o^2}{I_{C.G.}} \int_{-\frac{L}{2}}^{\frac{L}{2}} \lambda \lambda' \bar{x} \, dx \tag{4}$$

The thrust moment coefficient, C_2, was obtained from the following equation:

$$C_2 = \frac{\bar{X}_E F}{I_{CG.}} \tag{5}$$

where F is the thrust of the swivel engines. Equations 2 through 5 were obtained from Reference 2.

For rigid body control, the equation of motion for the rotation of a space vehicle may be written as (c.f. Reference 1)

$$\ddot{\varphi} + C_1\alpha + C_2\beta = 0 \tag{6}$$

providing translation and sloshing are not present. Assuming no wind, $\alpha =$; therefore,

$$\ddot{\varphi} + C_1\varphi + C_2\beta = 0 . \tag{7}$$

The simplified control equation can be written as:

$$\beta = a_o\varphi + a_1\dot{\varphi} . \tag{8}$$

Substituting equation (8) into (7)

$$\ddot{\varphi} + C_2a_1\dot{\varphi} + \left[C_1 + C_2a_o\right]\varphi = 0 . \tag{9}$$

It is evident from equation (9) that, for C_1 negative, the stability of the vehicle is decreased; however, as long as $C_1 + C_2$ is positive, stability is insured providing $C_2a_1 \geq 0$. Since C_2 is always positive, a_1 must be positive also for stability. For the vehicles studied in this investigation, all values of C_1 are negative. This indicates that the normal lift force, N', acts at a point forward to the total C. G. of the vehicle and produces a nose-up or destabilizing m moment. The fact that the C_P is located forward of the total vehicle C. G. is due to the truncated cone and nose cone surfaces which are also forward of the C. G. of each vehicle. This aerodynamic instability can, however, be eliminated by using engines which can be gimballed to produce a stabilizing moment about the vehicle's C. G. The thrust moment coefficient C_2, then, is a measure of this stabilizing moment as defined by equation (5).

It can be seen that C_2/C_1 is an indication of the aerodynamic stability of the vehicle. The greater C_2 and the smaller C_1, the more stable the vehicle. To eliminate negative values of the parameter C_2/C_1, the absolute value to C_1 will be used as shown in Figure 1. Also, the first bending mode frequency divided by the square root of the absolute value of C_1 is graphed in Figure 1. Since large bending frequencies are desirable from the control and sloshing point of view and since a small value for C_1 is desirable, the vehicle with the larger $f_1/\sqrt{|C_1|}$ is the more desirable vehicle, structurally and aerodynamically. As a matter of interest, an arbitrary shape parameter ($D_w^3 \frac{t}{L}$) was chosen in an effort to linearize the natural structural bending frequencies. This parameter is plotted against bending frequencies in Figure 4. The weighted diameter of the vehicle, D_w, was obtained from equation (10):

$$D_w = \frac{D_1 l_2}{L} + \frac{D_1 l_2}{L} + \frac{(D_1 + D_2)}{2} \frac{l_3}{L} + \cdots \frac{D_n l_n}{L} \tag{10}$$

$$= \frac{1}{L}\left[\frac{D_1 l_2}{2} + D_1 l_2 + \frac{(D_1 + D_2)}{2} l_3 + \cdots D_n l_n\right]$$

where $\frac{D_1}{2}$ is the average diameter of the nose cone, l_1 is the length of the cone, l_2 is the length of the section of vehicle behind the nose cone where D_1 is constant, etc. Figure 4 enables anyone to determine the first three bending frequencies for any vehicle merely be calculating the $D_w^3 \frac{t}{L}$ parameter; however, the weight and internal volume of the vehicle must be the same as the Saturn used in this report.

To determine C_1, C_2, and N', the maximum dyanmic pressure for the C-1 trajectory was used, which is

$$q_{MAX} = 6.54 \text{ lbs/in}^2 .$$

The thrust from the swivel engines was

$$F = 4(188,000) = 752,000 \text{ - lbs} .$$

The following table contains the data relevant to this investigation.

TABLE I

Bending and Aerodynamic Stability Data

Variables*	Vehicle 0	Vehicle 1	Vehicle 2	Vehicle 3	Vehicle 4	Vehicle 5
f_1	1.237	2.642	0.595	0.308	0.068	0.588
f_2	2.806	5.540	1.498	0.956	0.186	1.533
f_3	4.981	8.409	2.711	2.05	0.361	2.790
$\bar{X}_{IR}$	-385.4	-284.0	-595.7	-732.5	-1149.6	-500.0
$\bar{X}_{MC}$	335.7	151.8	454.9	600.9	54.7	213.0
m	7160	7101	7084	7165	7150	7100
t	0.210	0.231	0.179	0.126	0.113	0.172
L	2220	1730	2940	3096	6798	3000
$I_{CG} \times 10^{-9}$	1.86078	1.23674	3.88292	4.44662	26.66419	4.5716
C_P	-655.6	-700.5	-401.0	-481.0	-3308	-1393
N'	694,100	694,100	694,100	694,100	147,856	362,133
$\bar{X}_E$	674.3	613.3	920.1	847.1	3244.3	1287
C_1	-0.232	-0.394	-0.0717	-0.0752	-0.0184	-0.108
C_2	0.273	0.373	0.178	0.143	0.915	0.211
$C_2 / \lvert C_1 \rvert$	1.174	0.946	2.486	1.906	49.628	1.955
$f_1 / \sqrt{\lvert C_1 \rvert}$	2.566	4.207	2.220	1.124	0.500	1.789
$\bar{X}_{IR}/L$	-0.1736	-0.1642	-0.2026	-0.2366	-0.1691	-0.1667
D_w	195	225	172	162	116	177
$\frac{D_w^3 t}{L}$	701	1521	310	173	26	320

*Units are in the inch-pound-second system.
$\bar{X}_{IR}$ and C_P are measured from the C.G. of the vehicle.

The node points for the first bending mode of each missile are given in Table II below. The location of each point is measured in per cent of total vehicle length aft of the nose. Figures 2 and 3 present the vehicle configurations in order of magnitude of their bending frequencies and aerodynamic stability decreasing and increasing, respectively.

TABLE II

NODE LOCATIONS

VEHICLE	1st NODE	2nd NODE
0	29.7%	79.7%
1	35.5%	80.9%
2	30.6%	83.0%
3	27.6%	83.2%
4	23.8%	77.6%
5	28.3%	78.8%

TYPICAL FIRST BENDING MODE SHAPE

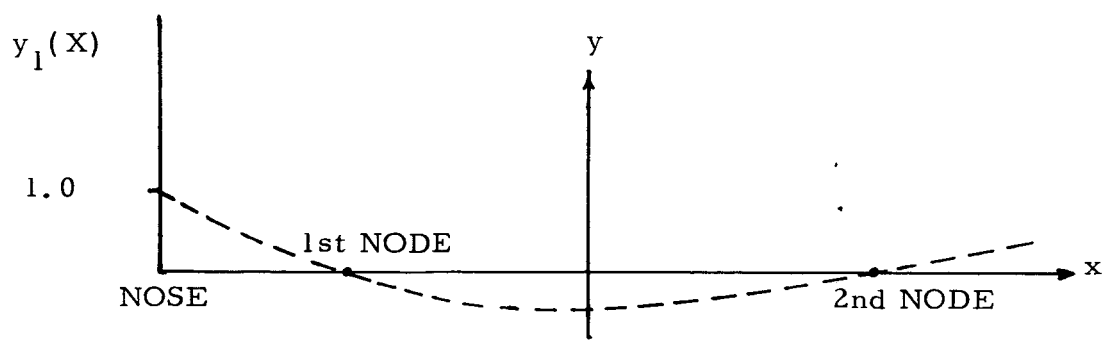

III. CONCLUSIONS

The graph of $C_2/|C_1|$ shown in Figure 1 indicates that this control-stability parameter increases rapidly after the vehicle length exceeds 3500 inches. This can be explained by the fact that each of the vehicles investigated has the same internal volume; therefore, its diameter decreases with an increase in length. This length increase decreases the normal lift force acting on the nose cone in proportion to the decrease in the square of base diameter of the vehicle. This causes C_1 to decrease but at the same $\bar{X}_p$ has become larger, thereby tending to increase C_1. However, $\bar{X}_E$ has been increased proportionally to the increase in $\bar{X}_p$. It should be stated that this is true only for single diameter vehicles such as numbers 1, 4, and 5. Since $\bar{X}_E$ occurs in C_2 and $\bar{X}_p$ in C_1, these two effects cancel and result in $C_2/|C_1|$ increasing at an exponential rate.

Although it is desirable for a vehicle to have its first bending mode frequency above the control and sloshing frequencies, which can be achieved with short vehicles, it is also necessary that any aerodynamic instabilities be controlled by swivel engines. The graph of $f_1/\sqrt{|C_1|}$ (Figure 1) illustrates the variation of this parameter with vehicle length and allows one to choose, when compared with the $C_2/|C_1|$ parameter, some compromise design between maximum bending frequency-minimum stability, and maximum stability-minimum bending frequency. Vehicles 1 and 4 are the extreme cases investigated here. For conical, single-diameter cylindrical, and dual-diameter cylindrical vehicles with the same approximate lengths, e.g., vehicles 2, 5, and 3, respectively, the conical vehicle exhibits more favorable bending and control characteristics than the other two, while the single-diameter cylindrical is better than the dual-diameter cylindrical vehicle.

Figure 4 illustrates the variation of the first three bending modes of each vehicle with the shape parameter, $D_w^3 \frac{t}{L}$. A linear relationship exists for the first mode for all values of shape parameter while the second mode is linear only for values of $D_w^3 \frac{t}{L}$ greater than 400. The third mode is nearly linear for $D_w^3 \frac{t}{L}$ greater than 500. The bending frequencies obtained for each vehicle are lower than those of an actual vehicle designed to the length and diameters specified in this report. This is due mainly to the way that the EI and mass distributions were obtained (see Description). The bending frequency of vehicle number zero is about 70 per cent of the actual frequency of SA-1 at lift-off.

It has been found that, when the propellant sloshing mass is located between the center of gravity and the center of instantaneous rotation of a vehicle, its stability is endangered; therefore, it is desirable to have these two positions located as close to each other as possible. Generally, the sloshing mass will be located aft of the vehicle center of gravity for first stage flight time and the center of instantaneous rotation forward of the C. G. From Table I it is seen that the more stable vehicles from this standpoint are, in descending order: 1, 5, 4, 0, 2, and 3. This is evidenced by the magnitude of $\bar{X}_{IR}/L$. In general, the smaller this value, the less the probability that an instability will occur due to sloshing, provided that the vehicle has only one sloshing mass, i. e., that sloshing masses of all other tanks are small in comparison to this one. It is also necessary that the sloshing masses be equal in each vehicle for the above statements to be true, which is not the case in the actual vehicle. For the small diameter vehicles, the sloshing mass is small, while for vehicles with large diameters the sloshing mass is dangerously large.

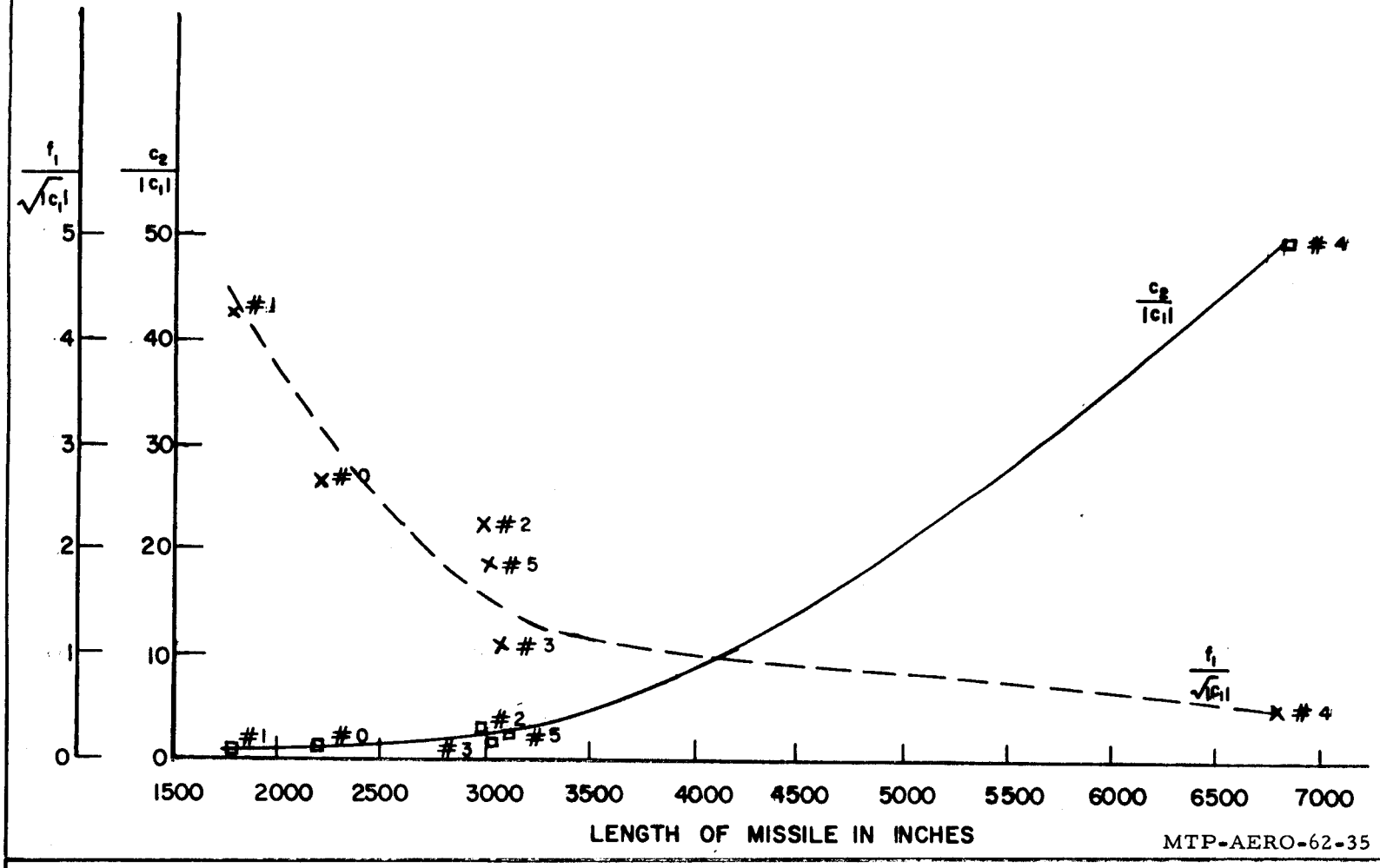

FIGURE I. FREQUENCY AND AERODYNAMIC STABILITY PARAMETER CURVES FOR THE VARIOUS CONFIGURATIONS

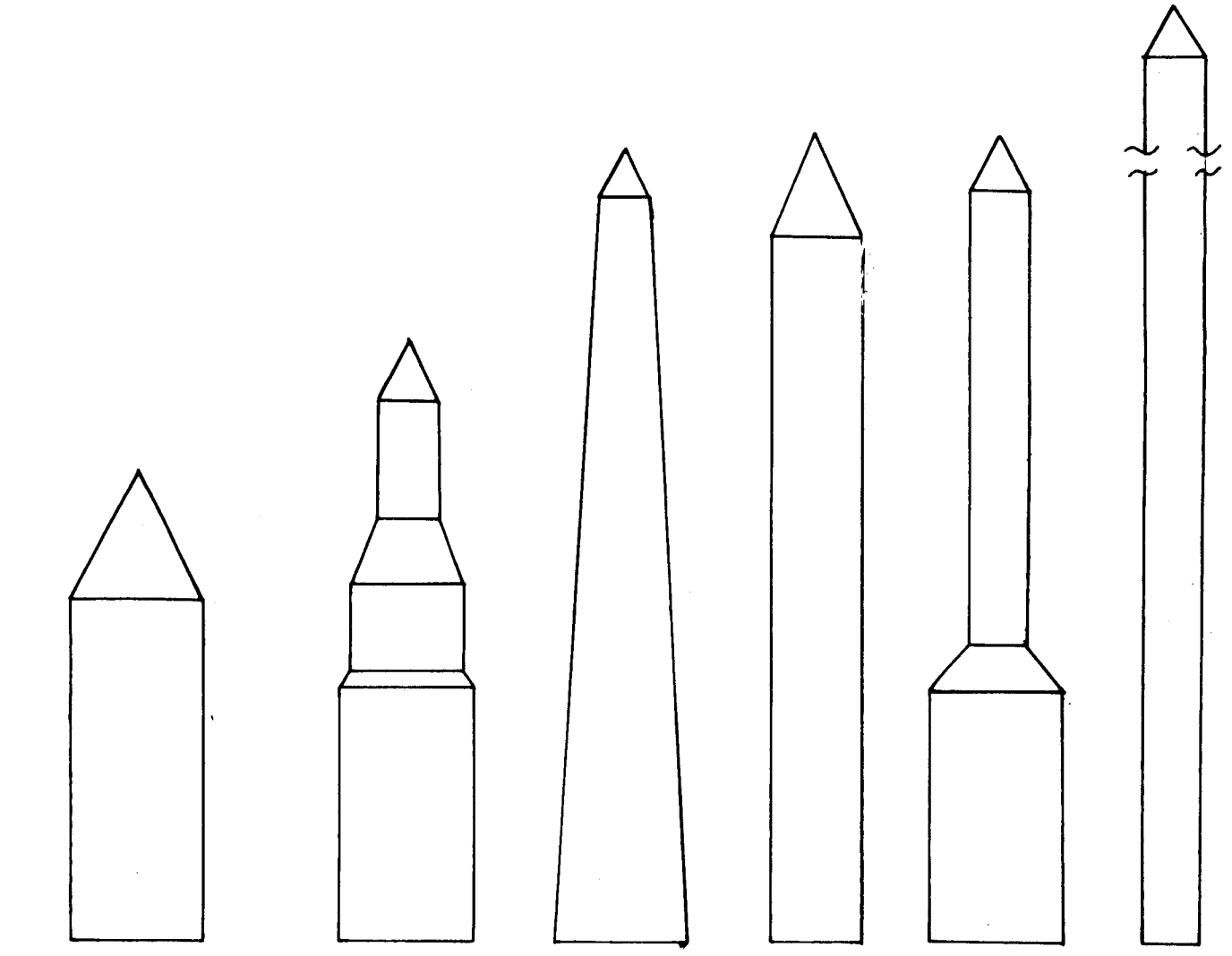

FIGURE 2. VEHICLE CONFIGURATIONS IN ORDER OF THEIR BENDING FREQUENCIES (DECREASING)

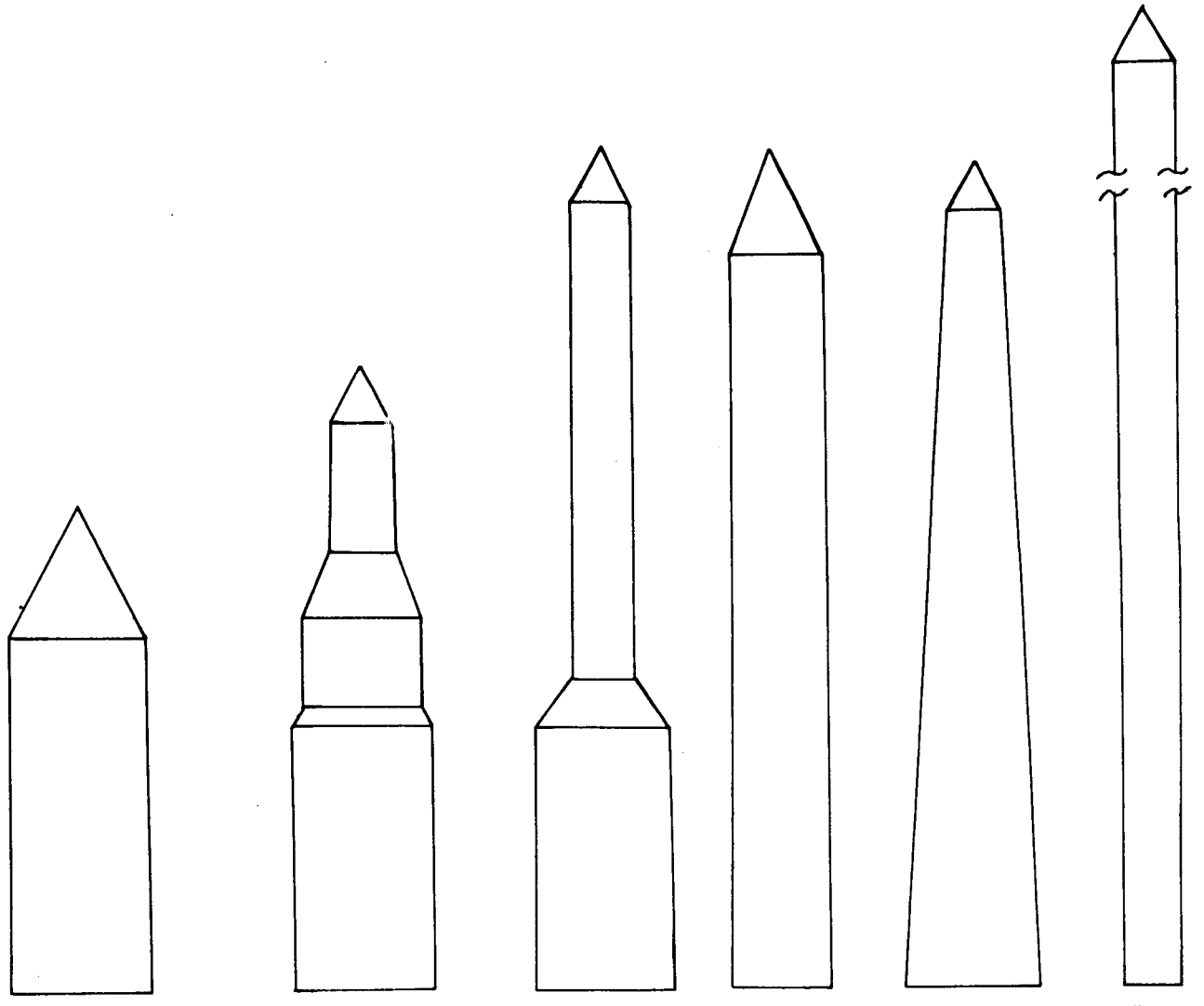

VEHICLE	#1	#0	#3	#5	#2	#4
C_2/C_1	0.95	1.17	1.91	1.96	2.49	49.60
LENGTH	1730"	2220"	3096"	3000"	2940"	6798"

FIGURE 3. VEHICLE CONFIGURATIONS IN ORDER OF THEIR AERODYNAMIC STABILITY (INCREASING) MTP-AERO-62-35

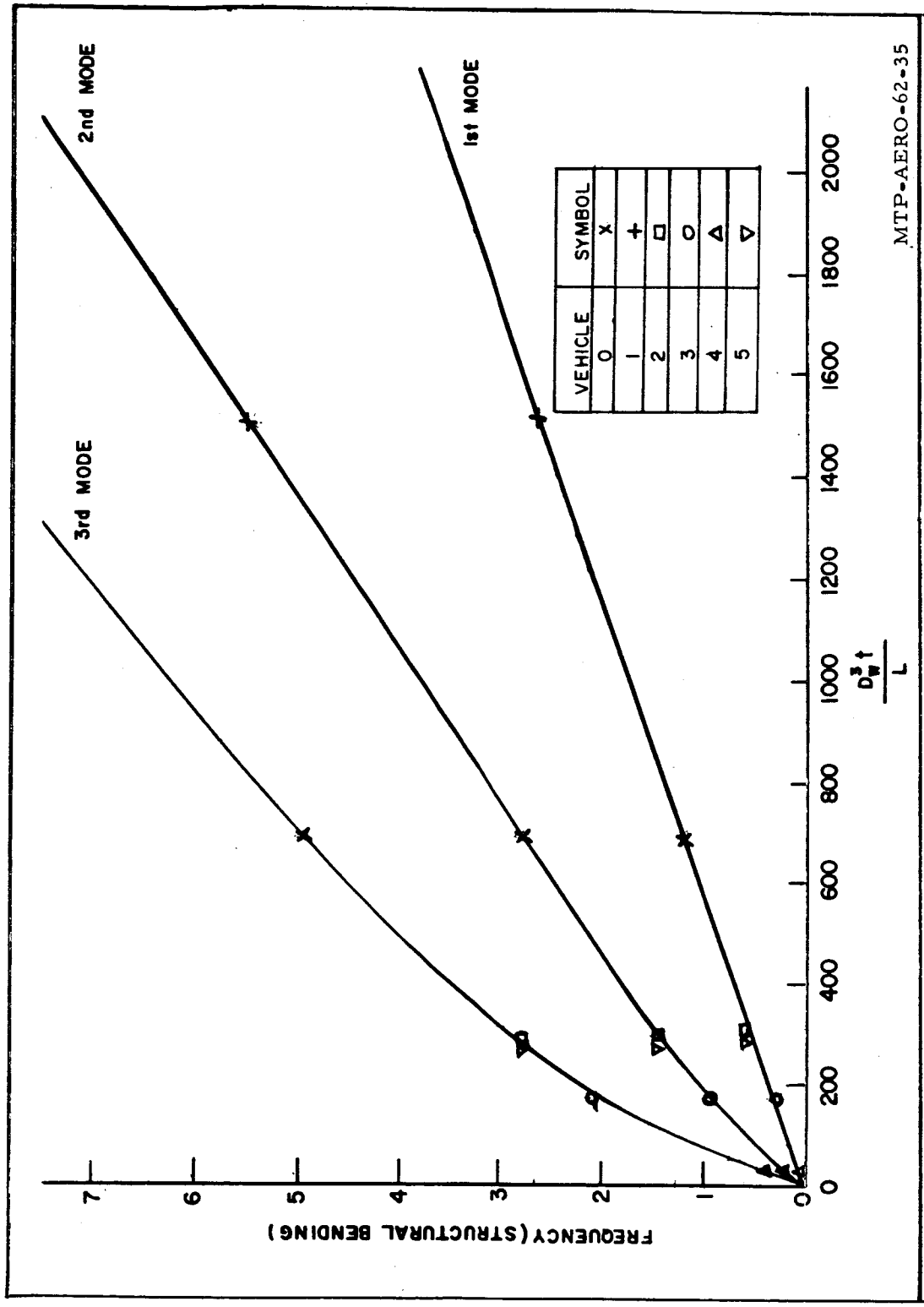

FIGURE 4. BENDING FREQUENCY VS SHAPE PARARMETER CURVES FOR THREE MODES

APPENDIX A

The first three bending mode deflection curves for each vehicle are given in this appendix.

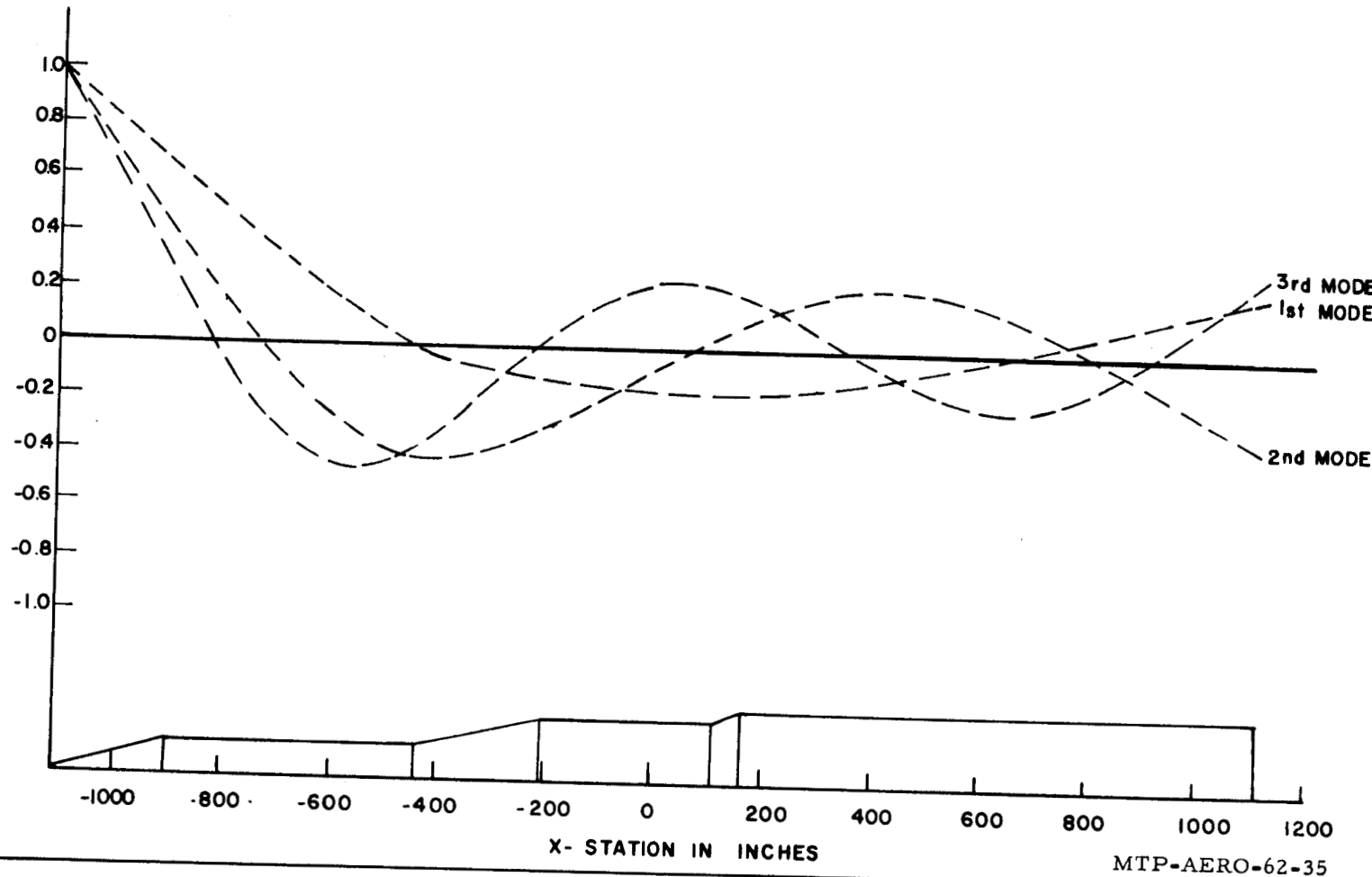

FIGURE 5. BENDING MODE DEFLECTION CURVES
FOR CONFIGURATION #0

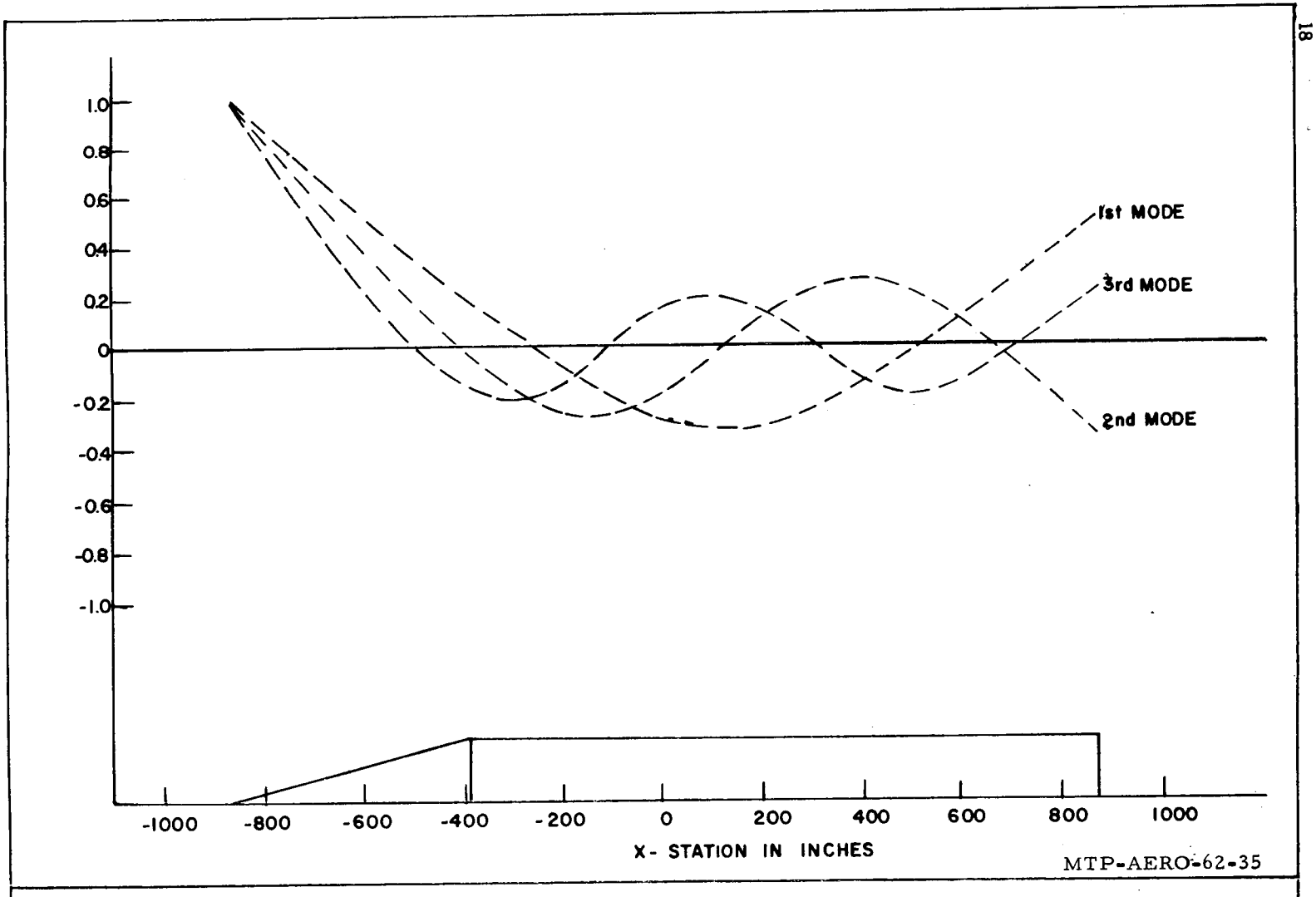

FIGURE 6. BENDING MODE DEFLECTION CURVES
FOR CONFIGURATION #1

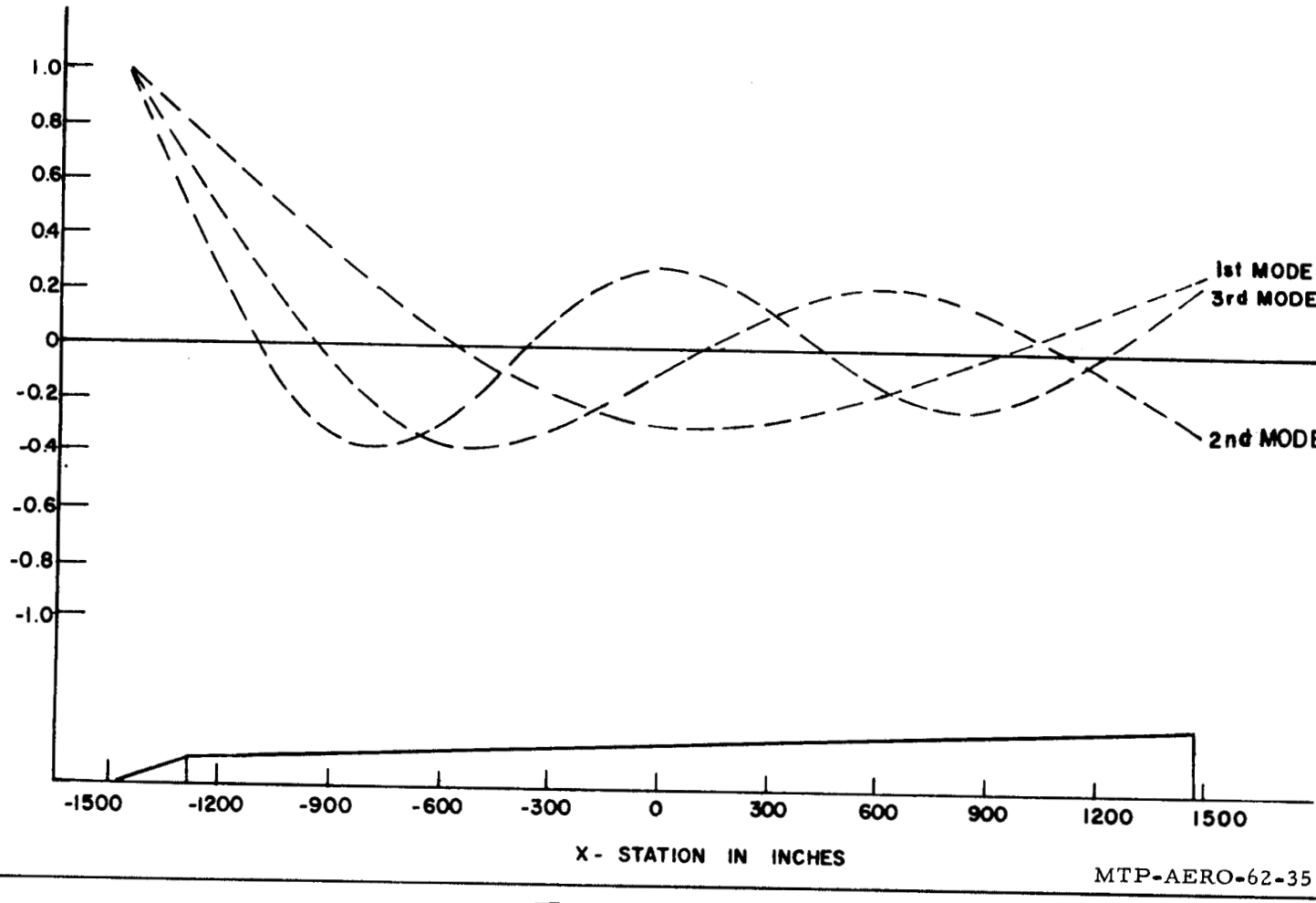

FIGURE 7. BENDING MODE DEFLECTION CURVES FOR CONFIGURATION #2

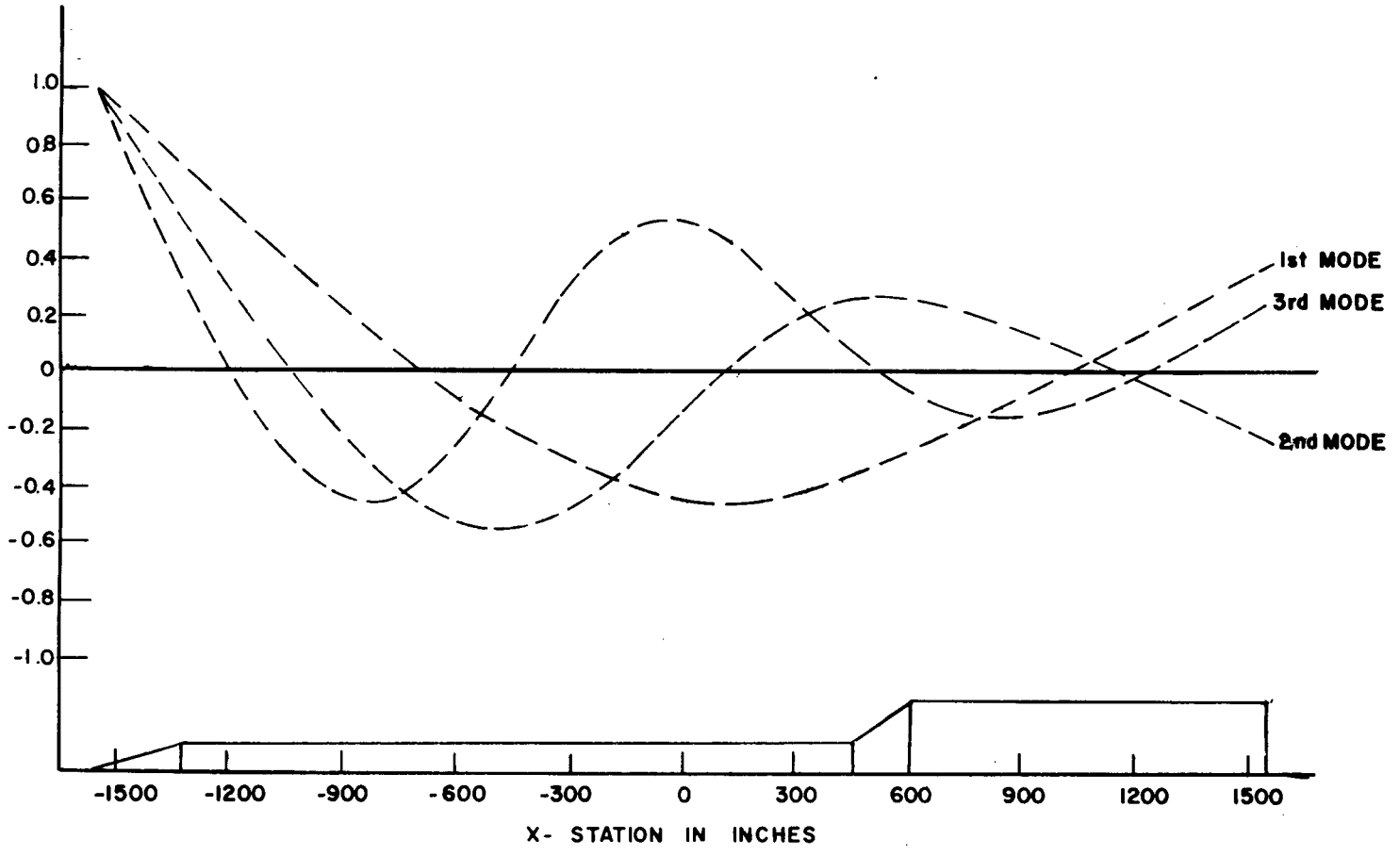

FIGURE 8. BENDING MODE DEFLECTION CURVES
FOR CONFIGURATION #3

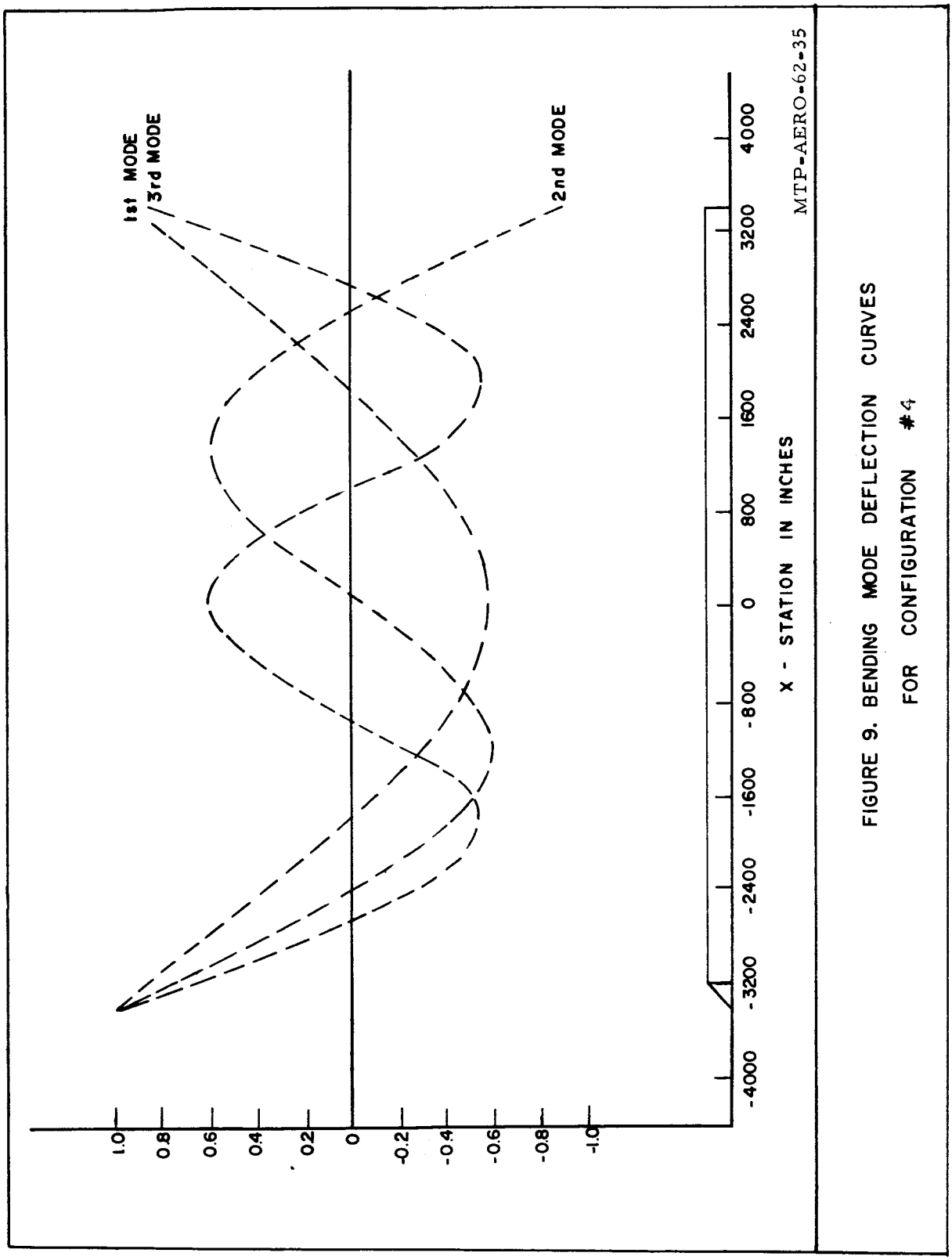

FIGURE 9. BENDING MODE DEFLECTION CURVES FOR CONFIGURATION #4

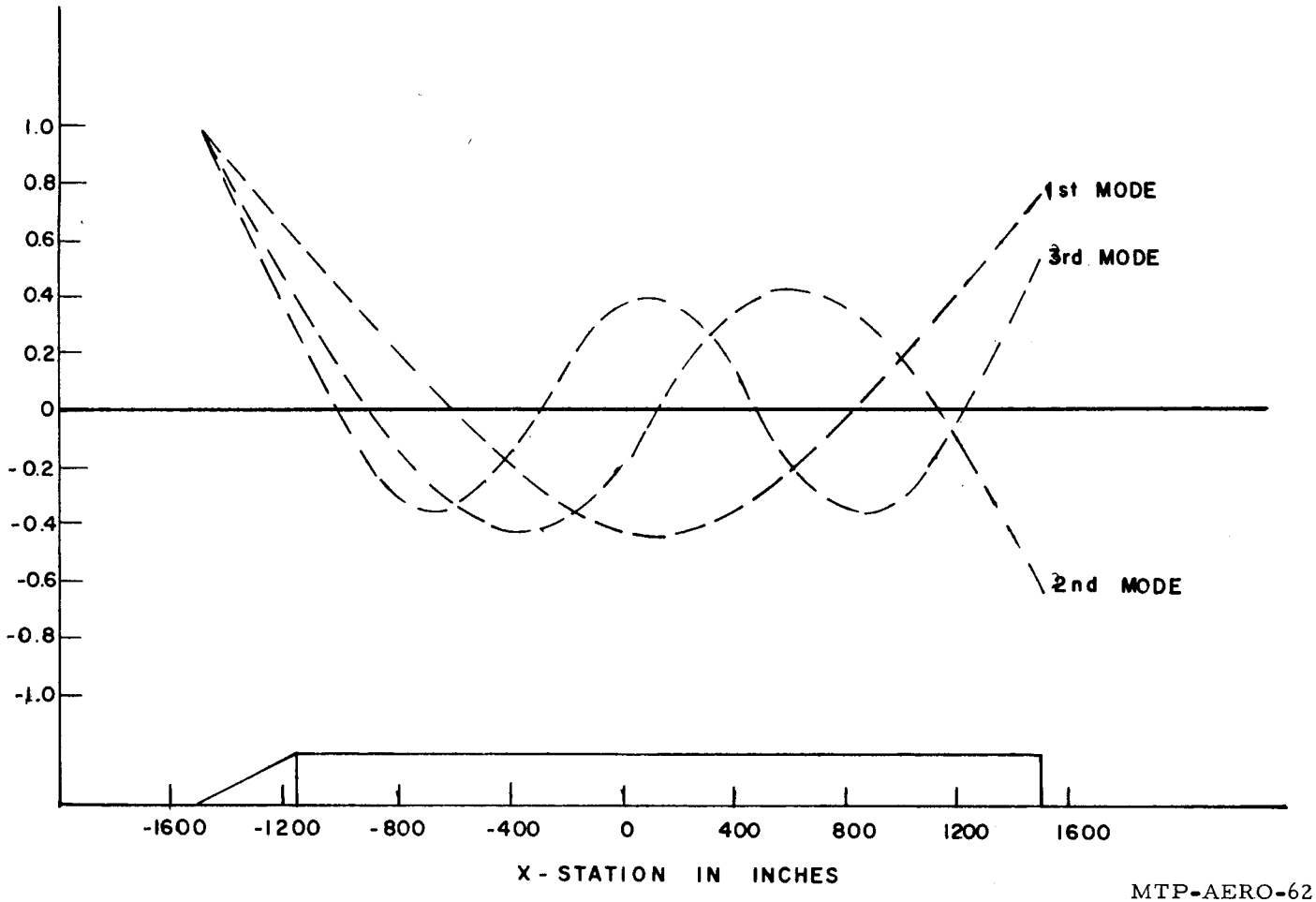

FIGURE 10. BENDING MODE DEFLECTION CURVES FOR CONFIGURATION #5

APPENDIX B

The mass distributions both empty and full for each configuration are contained in this appendix.

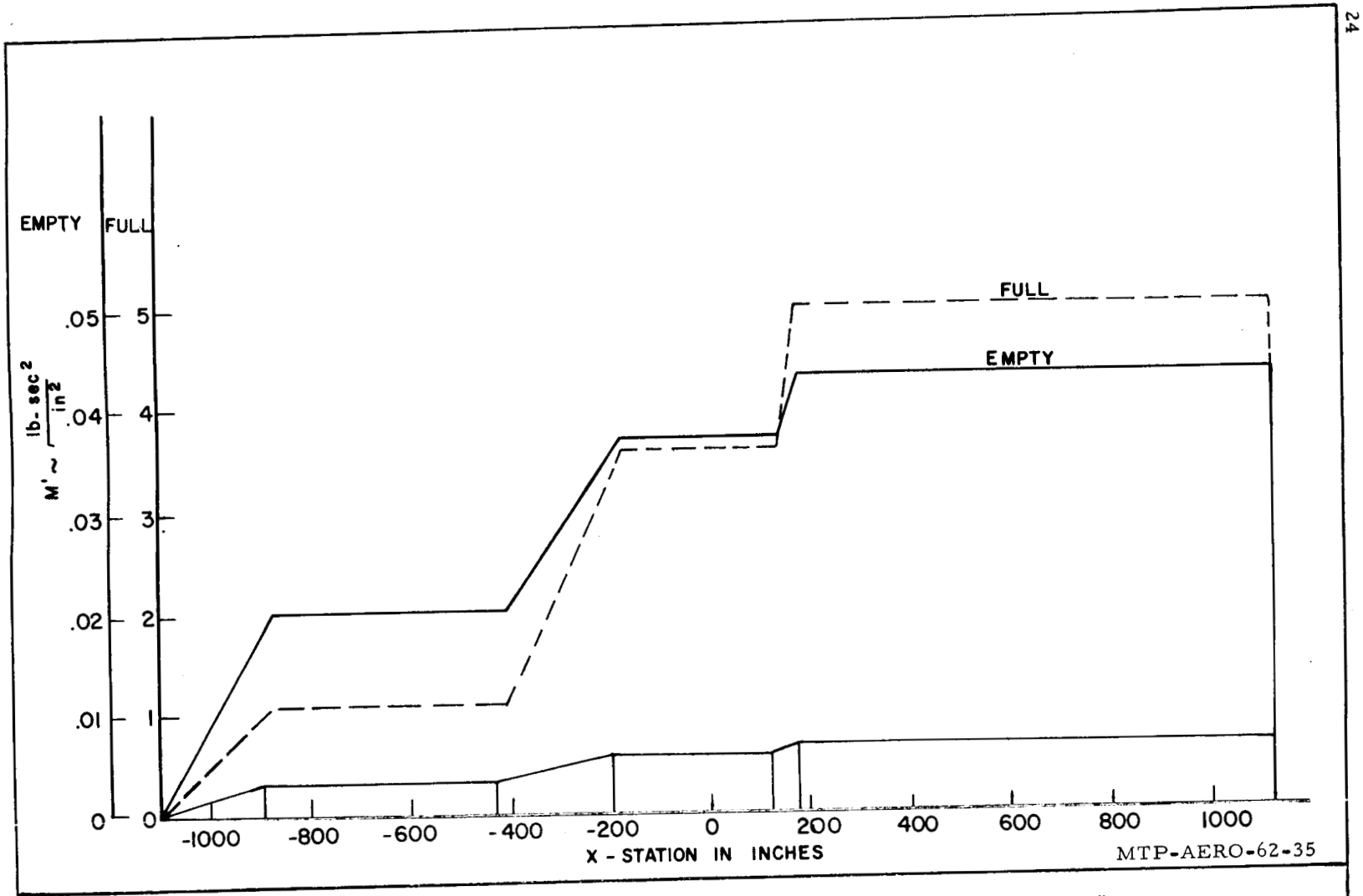

FIGURE II. MASS DISTRIBUTION FOR CONFIGURATION #0

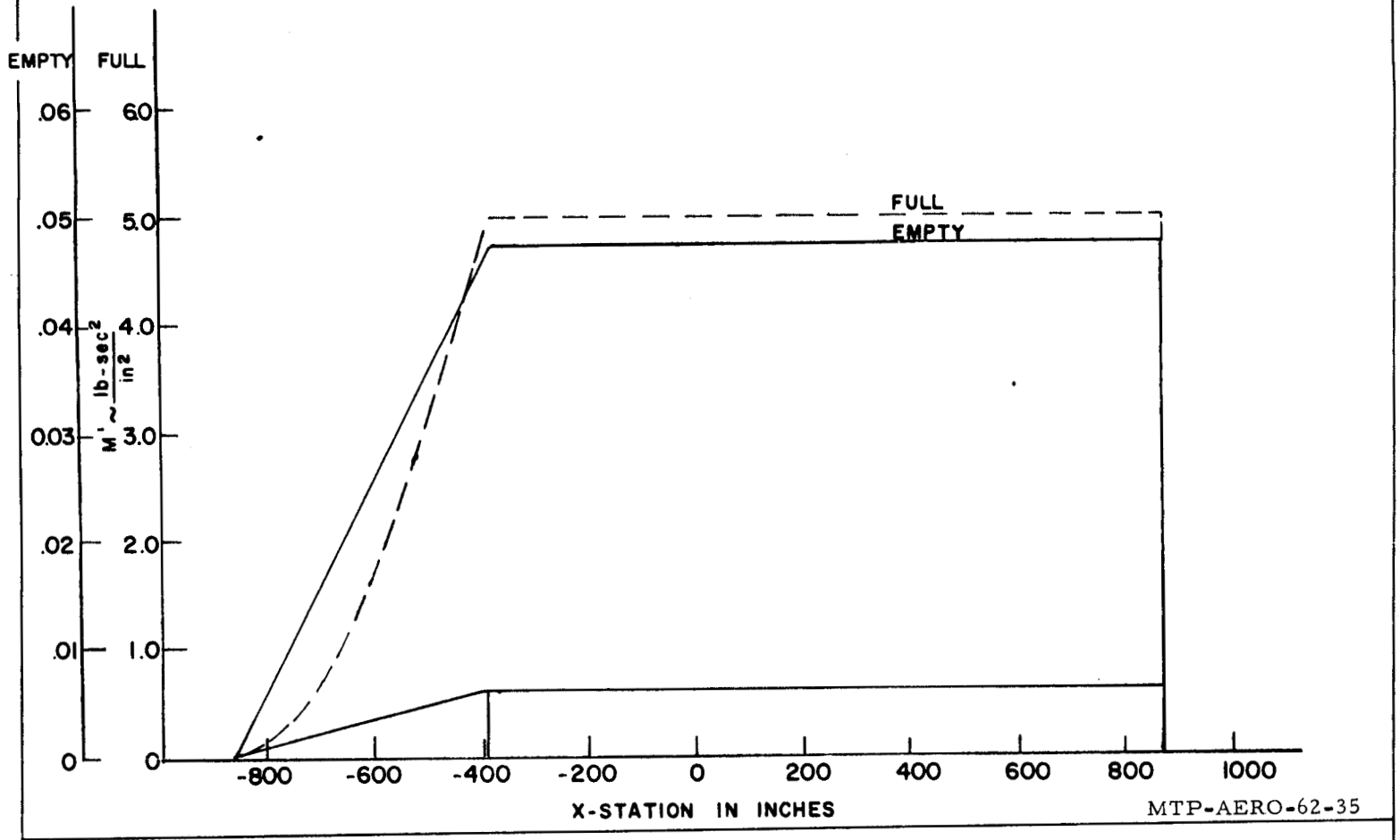

FIGURE 12. MASS DISTRIBUTION FOR CONFIGURATION # 1

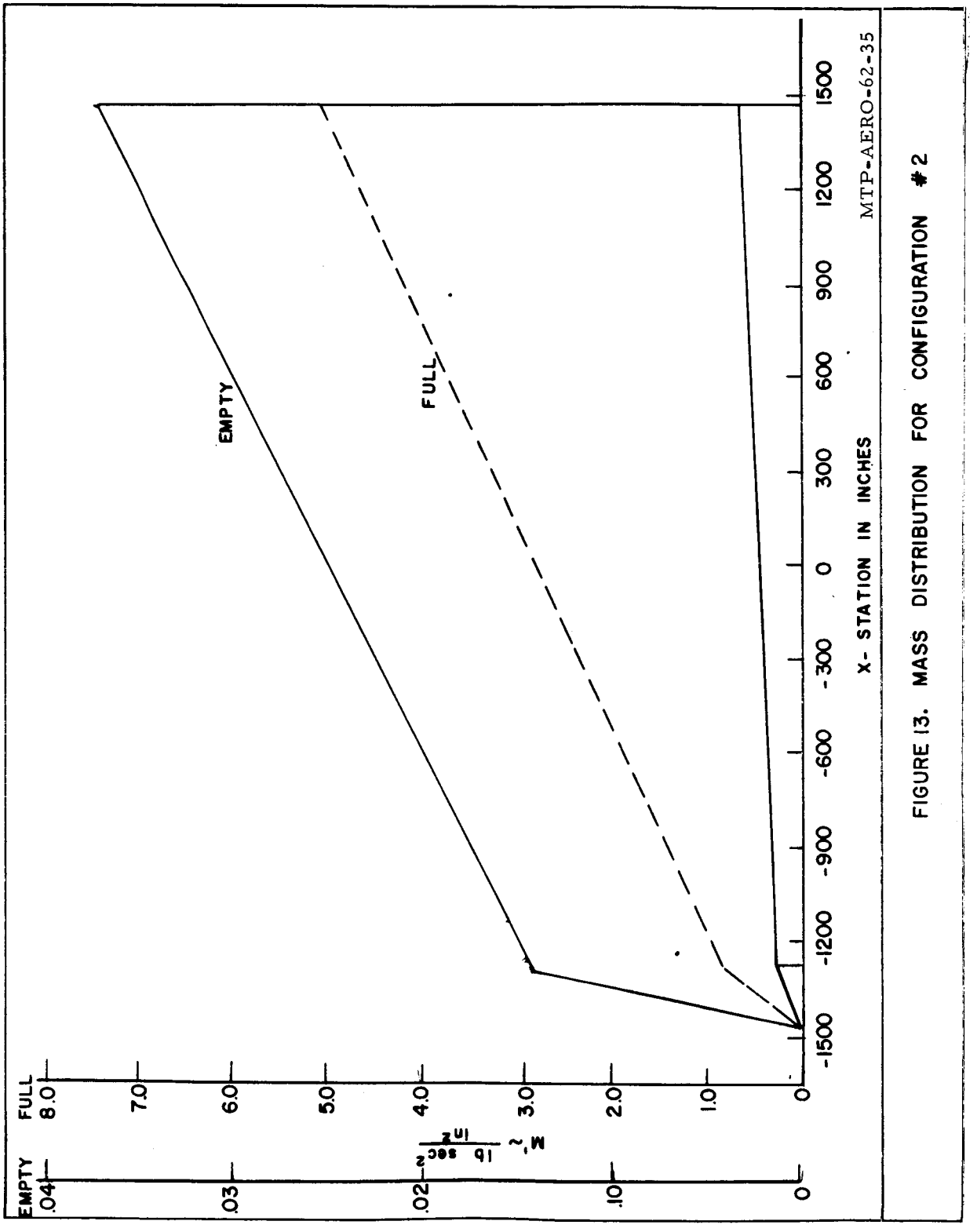

FIGURE 13. MASS DISTRIBUTION FOR CONFIGURATION #2

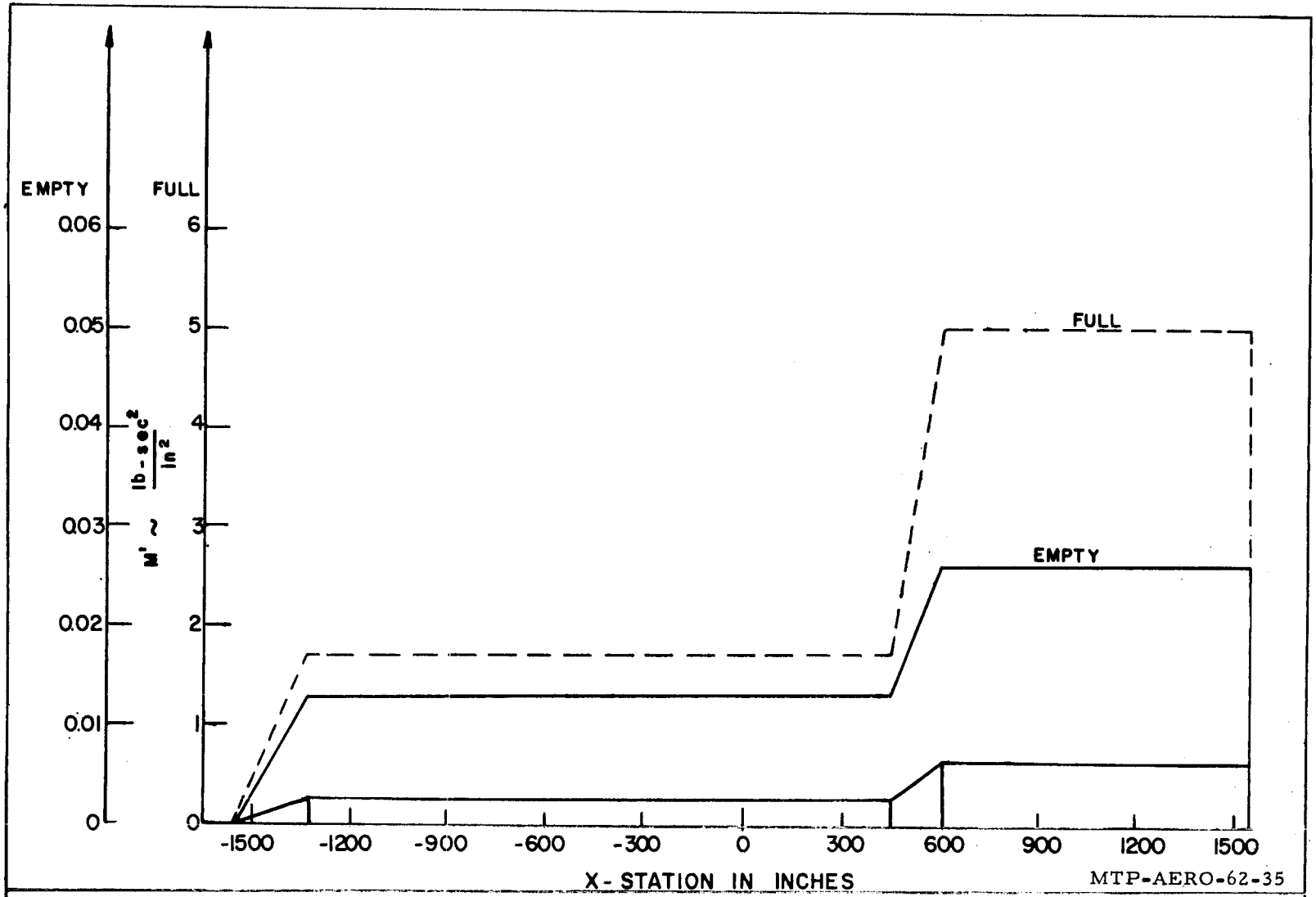

FIGURE 14. MASS DISTRIBUTIONS FOR CONFIGURATION #3

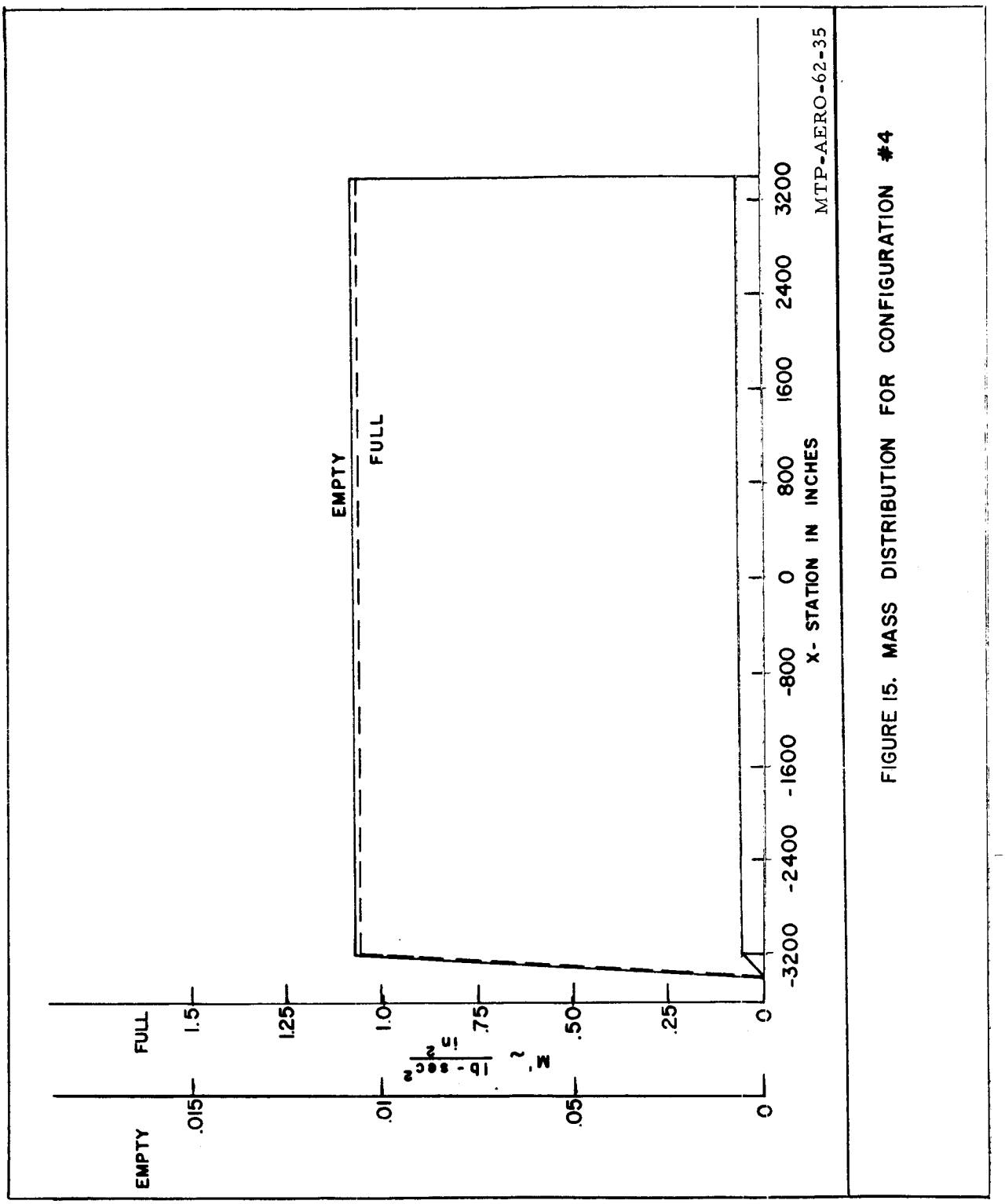

FIGURE 15. MASS DISTRIBUTION FOR CONFIGURATION #4

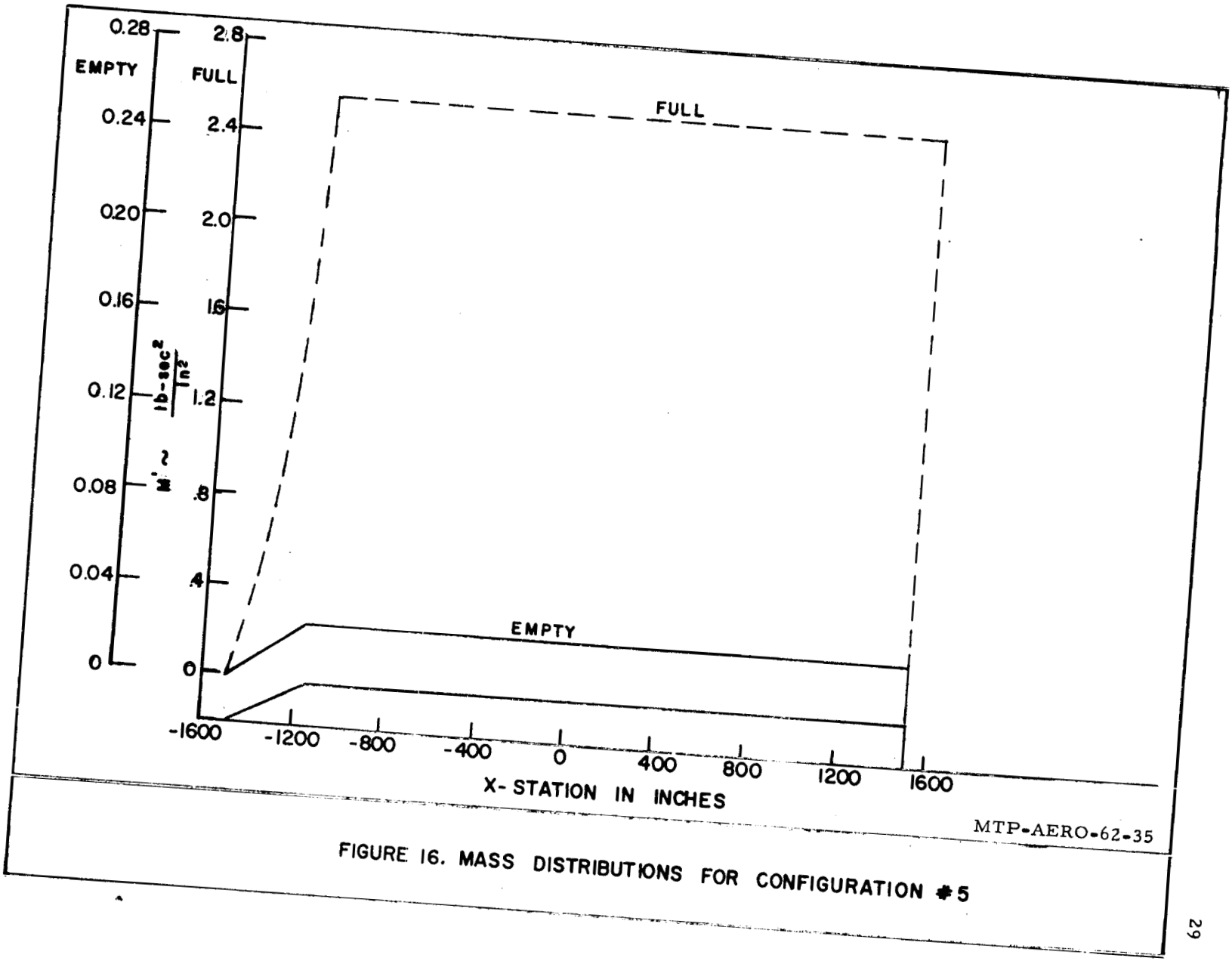

MTP-AERO-62-35

FIGURE 16. MASS DISTRIBUTIONS FOR CONFIGURATION #5

REFERENCES

1. Hoelker, R. H., Theory of Aritificial Stabilization of Missiles and Space Vehicles with Exposition of Four Control Principles. NASA TN D-555 June 1961.

2. Rheinfurth, Mario H., Control Feedback Stability Analysis. ABMA Report DA-TM 4-60.

3. Rheinfurth, Mario H., Modified Stodola Method Including Rotary Inertia and Shear Flexibility. ABMA Report DA-TR-4-59.

APPROVAL MTP-AERO-62-35

A THEORETICAL INVESTIGATION OF THE EFFECTS OF THE CONFIGURATIVE DESIGN OF A SPACE VEHICLE ON ITS STRUCTURAL BENDING FREQUENCIES AND AERODYNAMIC STABILITY

by NATHAN L. BEARD

The information in this report has been reviewed for security classification. Review of any information concerning Department of Defense or Atomic Energy Commission programs has been made by the MSFC Security Classification Officer. This report, in its entirety has been determined to unclassified.

Helmut F. Bauer

HELMUT F. BAUER
Chief, Fluttler & Vibration Section

HELMUT J. HORN
Chief, Dynamics Analysis Branch

E. D. GEISSLER
Director, Aeroballistics Division

DISTRIBUTION

M-DIR
- Dr. von Braun
- Dr. Rees

M-SAT
- Dr. Lange

M-COMP
- Dr. Hoelzer
- Dr. Fehlberg
- Dr. Schulz-Arenstorff
- Miss Morgan
- Miss Bostick

M-ME-M
- Dr. Kuers
- Mr. Wuenscher

M-ASTR
- Dr. Haeussermann
- Mr. Hosenthien
- Mr. Moore
- Mr. Digesu

M-LOD
- Dr. Debus
- Dr. Gruene
- Dr. Knothe

M-RP
- Dr. Stuhlinger
- Mr. Miles
- Mr. Dowdy

M-TEST
- Dr. Heimburg
- Dr. Tessman
- Mr. Pauli
- Dr. Sieber
- Mr. Haukohl
- Mr. Schuler

M-P&VE
- Dr. Mrazek
- Dr. Weidner
- Mr. Hellebrand
- Mr. Kroll

M-PAT

M-HME-P

M-H

M-MS-IPL (8)

M-MS-IP

- Mr. Paul
- Mr. Palaoro
- Mr. Heusinger
- Mr. Schulze
- Mr. Hein
- Mr. Hunt (2)
- Mr. Voss
- Mr. Bergeler
- Mr. Neighbors
- Mr. Goener
- Mr. Head

M-AERO
- Dr. Geissler
- Dr. Hoelker
- Mr. Horn
- Mr. Dahm
- Mr. Reed
- Dr. Speer
- Mr. Bauer
- Mr. Rheinfurth
- Mr. Ryan
- Mr. Hart
- Mr. Golmon
- Mr. Stone
- Mr. Baker
- Mrs. Chandler
- Mr. Larsen
- Mr. Thomae (2)
- Mr. Verderaime
- Mr. Kiefling
- Mr. Pack
- Mr. Grissett
- Mr. Scott
- Mr. Vaughan
- Mr. Harcrow
- Mr. Douglas
- Mr. Beard (20)
- Mr. W. W. Vaughan
- Mr. Scoggins